Dual Estimation of Attitude and Parameters Considering Vibration based on GPS and IMU

XIN Qi[1] , SHI ZhongKe[1] , ZHU HongYu[2]
1. School of automation, Northwestern Polytechnical University, Xi'an 710072, China
E-mail: shizknwpu@126.com
2. Norinco Group, North General Electronics Group Co., Ltd, Xi'an 710100, China

Abstract: Attitude determination is strongly coupled with the estimation of unknown vibration parameters when the output of the inertial measurement unit (IMU) is corrupted by the vibration induced by the piston engine. The unknown vibration parameters in the attitude dynamics can degrade attitude accuracy of dead reckoning. In this paper, a dual estimation of attitude and parameters considering vibration is investigated for small UAV. The dynamic model contained attitude and parameters is established by state augmentation, and the observations are chosen as GPS velocity and heading. In order to employ hybrid extended kalman filter for dual estimation, Jacobian matrixes are formulated by linearizing the estimation model to propagate and update error variance. Since joint state estimation has tremendous computational loads, based on matrix blocking a state and parameter separated estimation is proposed to decouple the estimation of attitude and parameters. Simulation results show that the proposed method can give high precision attitude than the common filter without considering vibration.

Key Words: flight mechanics, attitude determination, inertial measurement unit (IMU), dual estimation, vibration parameters

1 Introduction

Attitude determination is an essential process for flight dynamics, flight kinematics and maneuverability [1]. For instance, accidents always occurred when the reference attitude deviated from the normal state for autonomous navigation aircraft. Due to their size and power consumption, inertial measurement devices with a high precision are not suitable for small Unmanned aerial vehicle（UAV）. With the rapid developments of Micro Electro Mechanical System （MEMS) IMU and Global Positioning System（GPS）, the integrated attitude determination system (ADS) combined with MEMS IMU and GPS occupies a small volume, consumes low power, and provides high reliability solution , which is suitable for small UAV's attitude determination[2, 3]. However, ADS confronts two principal problems. Firstly, velocity and attitude given by dead reckoning system are based on acceleration and angular rate. The dead reckoning system works well only when there is no acceleration bias and no angular rate bias, while for the real dead reckoning system, serious drifts over time happen frequently [4, 5] since bias is always induced with changes of operating conditions. Secondly, without observation of horizontal attitude, the precision of attitude estimation greatly relies on the resolution of the acceleration and velocity when GPS and accelerometer are applied to revise ADS. Contrast to the large aircraft, the output of IMU is prone to be corrupted by the force-induced vibration when the small UAV is propelled by the piston engine. Researches show that accelerometer is more sensible to vibration than gyroscope [6].

With the availability of gyroscope, accelerometer, magnetometer, air data sensors, GPS, altimeter, cameras, radar, *et al,* inexpensive ADS with small size have been manufactured after Considerable efforts. The widely used ADS, attitude and heading reference system (AHRS), is composed of a tri-axial gyroscope, accelerometer and magnetometer. Dynamic attitude is obtained from gyroscope by dead reckoning while static attitude is acquired from accelerometer and magnetometer by solving Wahba's problem[5, 7, 8]. With the fusion of dynamic and static attitude, good attitude determination performance can be gotten by ADS under the condition that the observations of the accelerometers are the projections of gravity in the body-fixed coordinate system. The horizontal attitude, determined by ADS, will deviate from the truth when the condition is not satisfied. Moreover, two types of principal gyro-free ADSs are developed simultaneously, one is based on accelerometer array and the other is based on GPS. The accelerometer array based ADSs consist of more than sixes accelerometers installed on special space orientation for equivalent measurement of time derivative and magnitude of angular rate. ADS is prone to be divergent from the true attitude when there are some biases coupled in the equivalent measurements [6, 9]. The GPS-based ADSs determine attitude differently by the number of GPS antennas. Single antenna GPS can only determine what is called "pseudoattitude"[6, 10], while the true attitude needs more than 2 non-collinear antennas[2]. The multi-antennas GPS determines attitude by GPS antennas' relative location. The accuracy of ADS degrades greatly when installment errors of GPS antennas are pronounced or GPS signal is sheltered. Some approximated attitude determination methods are applied to steady state flight attitude determination as well. For instance, pitch angle can be determined by the air speed and altitude when the aircraft's principal motion is longitudinal [11].

Inertial Navigation System (INS)/GPS integrated navigation has attracted many researchers' attention. A loosely coupled INS/GPS is formed for location and velocity determination while a tightly coupled INS/GPS is formed for attitude estimation. Tightly coupled INS/GPS calibrates attitude drifts by the errors of velocity and heading. However, velocity given by dead reckoning may show some vibrations, as the filter regards acceleration vibration as part of the errors to compensate the horizontal attitude. As a consequence, the attitude determined by this method diverges from the truth for the incorrect compensation. For this problem, Jan and Shau-Shiun investigated an attitude

*This work is supported by National Natural Science Foundation (NNSF) of China under Grant 61143004.

978-1-4673-5769-2/13/$31.00 ©2013 IEEE

estimation method based on gyroscopes and single antenna GPS with vibration [6]. In that paper, spectrum analysis shows that the acceleration is damaged by vibration more severely than the angular rate, and the horizontal attitude determined by acceleration is less precise than "pseudoattitude" determined by GPS. Therefore, the solution for the attitude determination is implemented by GPS and gyroscope. However, there are some drawbacks about the ADS, especially that the "pseudoattitude" reflects the true attitude only at the situation of coordination flight.

If a perfect acceleration is available for the reckoning velocity, the attitude determined by GPS and accelerometer no longer needs any theoretic assumptions. The acceleration can be more accurate by the dual estimation of attitude and parameters with the dynamics of vibration parameters. The remainder of the paper is organized as follows. Section II describes the dynamics of velocity and attitude, as well as the characteristics of the coupled vibration. In section III, the estimation model is established with the measurement of the IMU corrupted by Gaussian white noise, bias and vibration. In order to improve the computing efficiency, state and parameters separated estimation is employed to implement dual estimation. In section IV, we show the experiment settings and results. Our conclusion is given in section V.

2 Problem Statement

Let c_α represent $\cos\alpha$, s_α represent $\sin\alpha$, and assuming that the angular rate of geodetic coordinates (North-East-Down, NED) relative to inertial coordinates is infinitely small, the dynamics of attitude (Roskam, 2001) in terms of Euler angles is described by the following equation.

$$\begin{cases} \dot{\phi} = p + (qs_\phi + rc_\phi)s_\theta / c_\theta \\ \dot{\theta} = qc_\phi - rs_\phi \\ \dot{\psi} = (qs_\phi + rc_\phi) / c_\theta \end{cases} \tag{1}$$

where, p , q , r denotes the rolling rate, pitching rate, yawing rate in the body-fixed coordinates, respectively. ϕ , θ , ψ denotes the roll attitude, pitch attitude and heading, separately. Generally, the velocity dynamics is the most relevant equation for the attitude determination, and its equations are given by Eq. (2).

$$\begin{cases} \dot{v}^n = g(n_x c_\psi c_\theta + n_y(c_\psi s_\theta s_\phi - s_\psi c_\phi) + n_z(c_\psi s_\theta c_\phi + s_\psi s_\phi)) \\ \dot{v}^e = g(n_x s_\psi c_\theta + n_y(s_\psi s_\theta s_\phi + c_\psi c_\phi) + n_z(s_\psi s_\theta c_\phi - c_\psi s_\phi)) \\ \dot{v}^d = g(-n_x s_\theta + n_y c_\theta s_\phi + n_z c_\theta c_\phi + 1) \end{cases} \tag{2}$$

where n_x , n_y and n_z represent axial acceleration, side acceleration and normal acceleration, respectively. g is gravitational acceleration. v^n , v^e and v^d denote the northern velocity, eastern velocity and down velocity in the geodetic coordinates, separately.

As shown in Eq. (2), the attitude can be drawn from the velocity and the acceleration. The horizontal attitude is well determined if the time derivative of velocity in the geodetic coordinates and the acceleration in the body-fixed coordinates are known. Therefore, the basic states are $[v^n\ v^e\ v^d\ \phi\ \theta\ \psi]^{\mathrm{T}}$, the observations are $[v^{nm}\ v^{em}\ v^{dm}\ \psi^m]^{\mathrm{T}}$, and the inputs are $[p^m\ q^m\ r^m\ n_x^m\ n_y^m\ n_z^m]^{\mathrm{T}}$. The outputs of IMU are always corrupted by the Gaussian white noise, unknown constant bias and vibration. The principal component of vibrations can be modeled as a simplex sinusoidal function. According to the forced vibration theorem, the Shannon sampling theorem and the users' manual of the widely used piston engine, the frequency of the vibration coupled in the outputs of the IMU is range from 3.33Hz to 18.33Hz, when IMU is sampled at 50Hz. *MaxInt* is defined by Eq. (3) to assess the maximum integration pulse introduced by the unit vibration.

$$MaxInt = \int_{t_0}^{t_0+T/4} \sin(2\pi ft + \varphi_0)dt = \frac{1}{\pi f} \tag{3}$$

Fig.1 shows the curve of *MaxInt* versus vibration frequencies. According to Fig.1, the lower the frequency is, the larger the *MaxInt* is. Though the *MaxInt* of the direct current component is greater than others, it runs rapidly to the steady state. On the contrary, the vibration convergence rate is quite slow. Therefore, the vibration continuously influences the attitude determination process.

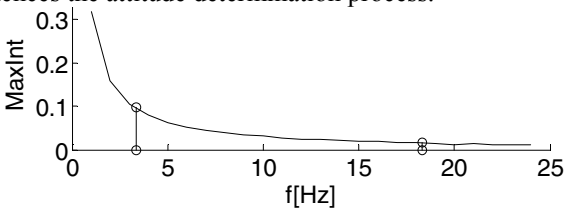

Fig.1 *MaxInt* versus vibration frequency

3 Dual Estimation of Attitude and Vibration

The dual estimation is widely used in the joint estimation of states and parameters. The structure of dual estimation for attitude and parameters shows in Fig.2. Bias and vibration are augmented as states in dual estimation, and the estimation of bias and vibration is feedback to calibrate the acceleration and the angular rate. If the bias and vibration are estimated with a sufficient accuracy, the attitude given by the dead reckoning will no longer drift over time or vibration with fast speed. Attitude determination models gradually coupled with Gaussian white noise, constant bias and vibration are discussed subsequently.

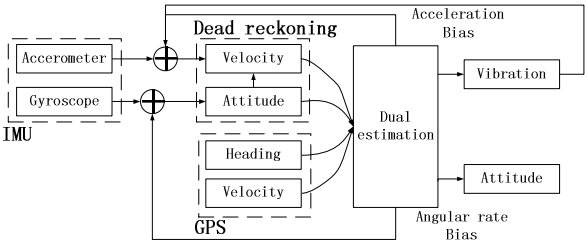

Fig.2 Dual estimation structure for attitude and parameters

3.1 Gaussian White Noise Corrupted IMU Outputs

As is known to all, observations are always corrupted by noises. Thus, the general dynamic and observation equation of a UAV is

$$\begin{cases} \dot{\boldsymbol{x}} = \boldsymbol{f}(\boldsymbol{x}, \boldsymbol{u}^{\mathrm{t}}) \\ \boldsymbol{z}_k = \boldsymbol{h}(\boldsymbol{x}_k) + \boldsymbol{\xi}_k \end{cases} \tag{4}$$

where, $\boldsymbol{u}^{\mathrm{t}}$ is the control input, always represented as $\boldsymbol{u}^{\mathrm{t}} = \boldsymbol{u}^{\mathrm{m}} + \boldsymbol{w}$, $\boldsymbol{u}^{\mathrm{m}}$ is the measurement of control input, and $\boldsymbol{w}$ is Gaussian white noise $[\omega_x\ \omega_y\ \omega_z\ \omega_p\ \omega_q\ \omega_r]^{\mathrm{T}}$. ω_x, ω_y , ω_z denote the tri-axial acceleration noises. ω_p , ω_q , ω_r denote the tri-axial angular rate noises. $\boldsymbol{z}_k$ is observation

$[v_k^{nm}\ v_k^{em}\ v_k^{dm}\ \psi_k^m]^{\mathrm{T}}$, which is corrupted by the Gaussian white noise $\boldsymbol{\xi}_k$. Then the UAV equations corrupted by noises are

$$\begin{cases} \dot{\boldsymbol{x}} = \boldsymbol{f}(\boldsymbol{x}, \boldsymbol{u}^{\mathrm{m}} + \boldsymbol{w}) \\ \boldsymbol{z}_k = \boldsymbol{h}(\boldsymbol{x}_k) + \boldsymbol{\xi}_k \end{cases} \tag{5}$$

The estimation model with control inputs corrupted by noises is established by Eqs. (1-2) and Eq. (5). The principal problem to determine the attitude is fusing the dead reckonings and the observations. Many filter based methods can be applied to nonlinear state estimation, such as EKF, UKF, DDF, CDF, GHF, PF, Neuron Networks and Kriging estimation[13-20]. Considering workhorse role of EKF in the real time state estimation, EKF is chosen to solve the problem. If $[v^n\ v^e\ v^d\ \phi\ \theta\ \psi]^{\mathrm{T}}$ is chosen as state, then the corresponding Jacobian matrices are calculated by linearizing Eq. (5).

Firstly, the partial derivative of $\boldsymbol{f}(\boldsymbol{x}, \boldsymbol{u}^{\mathrm{m}} + \boldsymbol{w})$ with respect to $\boldsymbol{x}$ at time $t_0 + (k-1)T$, is given in Eq. (6).

$$\boldsymbol{F} = \left.\frac{\partial \boldsymbol{f}}{\partial \boldsymbol{x}}\right|_{\hat{\boldsymbol{x}}_{k-1}} = \begin{bmatrix} \boldsymbol{0}_3 & \boldsymbol{F}_{12} \\ \boldsymbol{0}_3 & \boldsymbol{F}_{22} \end{bmatrix} \tag{6}$$

where $\boldsymbol{0}_n \in \boldsymbol{R}^{n\times n}$ and each element in $\boldsymbol{0}_n$ is 0. $\boldsymbol{F}_{12}$ and $\boldsymbol{F}_{22}$ are given in Eq. (7) and Eq. (8), respectively.

$$\boldsymbol{F}_{12} = \begin{bmatrix} f_{11} & f_{12} & f_{13} \\ f_{21} & f_{22} & f_{23} \\ f_{31} & f_{32} & 0 \end{bmatrix} \tag{7}$$

$$\boldsymbol{F}_{22} = \begin{bmatrix} (q\,\mathrm{c}_\phi - r\,\mathrm{s}_\phi)s_\theta / c_\theta & (qs_\phi + rc_\phi)/(c_\theta)^2 & 0 \\ -qs_\phi - rc_\phi & 0 & 0 \\ (q\,\mathrm{c}_\phi - r\,\mathrm{s}_\phi)/c_\theta & (qs_\phi + rc_\phi)s_\theta/(c_\theta)^2 & 0 \end{bmatrix} \tag{8}$$

The elements in Eq. (7) represent the contribution of the attitude towards the velocity, and its expressions are

$$\begin{cases} f_{11} = gn_y(c_\psi s_\theta c_\phi + s_\psi s_\phi) + gn_z(s_\psi c_\phi - c_\psi s_\theta s_\phi) \\ f_{12} = -gn_x c_\psi s_\theta + gn_y c_\psi c_\theta s_\phi + gn_z c_\psi c_\theta c_\phi \\ f_{13} = -gn_x s_\psi c_\theta - gn_y(s_\psi s_\theta s_\phi + c_\psi c_\phi) + gn_z(c_\psi s_\phi - s_\psi s_\theta c_\phi) \\ f_{21} = gn_y(s_\psi s_\theta c_\phi - c_\psi s_\phi) - gn_z(s_\psi s_\theta s_\phi + c_\psi c_\phi) \\ f_{22} = -gn_x s_\psi s_\theta + gn_y s_\psi c_\theta s_\phi + gn_z s_\psi c_\theta c_\phi \\ f_{23} = gn_x c_\psi c_\theta + gn_y(c_\psi s_\theta s_\phi - s_\psi c_\phi) + gn_z(c_\psi s_\theta c_\phi + s_\psi s_\phi) \\ f_{31} = gn_y c_\theta c_\phi - gn_z c_\theta s_\phi \\ f_{32} = -gn_x c_\theta - gn_y s_\theta s_\phi - gn_z s_\theta c_\phi \end{cases} \tag{9}$$

Secondly, the partial derivative of $\boldsymbol{f}(\boldsymbol{x}, \boldsymbol{u}^{\mathrm{m}} + \boldsymbol{w})$ with respect to $\boldsymbol{w}$ at time $t_0 + (k-1)T$, is shown in Eq. (10).

$$\boldsymbol{\Gamma} = \left.\frac{\partial \boldsymbol{f}}{\partial \boldsymbol{w}}\right|_{\hat{\boldsymbol{x}}_{k-1}} = \begin{bmatrix} \boldsymbol{\Gamma}_{11} & \boldsymbol{0}_3 \\ \boldsymbol{0}_3 & \boldsymbol{\Gamma}_{22} \end{bmatrix} \tag{10}$$

where $\boldsymbol{\Gamma}_{11} = g\begin{bmatrix} c_\psi c_\theta & c_\psi s_\theta s_\phi - s_\psi c_\phi & c_\psi s_\theta c_\phi + s_\psi s_\phi \\ s_\psi c_\theta & s_\psi s_\theta s_\phi + c_\psi c_\phi & s_\psi s_\theta c_\phi - c_\psi s_\phi \\ -s_\theta & c_\theta s_\phi & c_\theta c_\phi \end{bmatrix}$,

$$\boldsymbol{\Gamma}_{22} = \begin{bmatrix} 1 & s_\phi s_\theta / c_\theta & c_\phi s_\theta / c_\theta \\ 0 & c_\phi & -s_\phi \\ 0 & s_\phi / c_\theta & c_\phi / c_\theta \end{bmatrix}.$$

Finally, the partial derivative of $\boldsymbol{h}(\boldsymbol{x}_k)$ with respect to $\boldsymbol{x}$ at time $t_0 + kT$, is shown in Eq. (11).

$$\boldsymbol{H} = \left.\frac{\partial \boldsymbol{h}}{\partial \boldsymbol{x}}\right|_{\hat{\boldsymbol{x}}_{k,k-1}} \begin{bmatrix} \boldsymbol{E}_3 & \boldsymbol{0}_{3\times 2} & \boldsymbol{0}_{3\times 1} \\ \boldsymbol{0}_{1\times 3} & \boldsymbol{0}_{1\times 2} & 1 \end{bmatrix} \tag{11}$$

Where $\boldsymbol{E}_n$ denotes the $n\times n$ identity matrix.

3.2 Random Const Bias Coupled in IMU Outputs

The original output of MEMS IMU is represented by voltage, and a certain explicit mapping function needs to be employed to reconstruct the smoothing acceleration and the angular rate. Though some empirical formula obtained by a turn-table calibration is suitable to approximate the explicit mapping function, the mapping accuracy of the empirical formula is strongly correlated with the calibration method, calibration device, and the calibration state of IMU. The mapping errors are induced by the empirical formula when the zero state of the IMU drifts, such as temperature induced drifts, voltage supply induced drifts, *et al*, and relation for drift is quite hard to establish. In order to compensate the drift, it is rational to assume that the drift is a constant bias vector. Therefore, the input of the dead reckoning process is modeled by $\boldsymbol{u}^{\mathrm{t}} = \boldsymbol{u}^{\mathrm{m}} + \boldsymbol{\delta u} + \boldsymbol{w}$, where, $\boldsymbol{\delta u}$ denotes the bias vector in the input.

The attitude and the velocity obtained by the dead reckoning is vulnerable to the bias, since the divergence of dead reckoning is always caused by the bias. Augmenting the bias to the state for the dual estimation of attitude and velocity is essential. Using the bias estimation to calibrate the output of IMU will prevent divergence. When $[v^n\ v^e\ v^d\ \phi\ \theta\ \psi\ \delta n_x\ \delta n_y\ \delta n_z\ \delta p\ \delta q\ \delta r]^{\mathrm{T}}$ is set as the state, the corresponding Jacobian matrices for the error variance propagation and update is changed as Eq. (12).

$$\boldsymbol{F} = \begin{bmatrix} \boldsymbol{0}_3 & \boldsymbol{F}_{12} & \boldsymbol{\Gamma}_{11} & \boldsymbol{0}_3 \\ \boldsymbol{0}_3 & \boldsymbol{F}_{22} & \boldsymbol{0}_3 & \boldsymbol{\Gamma}_{22} \\ \boldsymbol{0}_3 & \boldsymbol{0}_3 & \boldsymbol{0}_3 & \boldsymbol{0}_3 \\ \boldsymbol{0}_3 & \boldsymbol{0}_3 & \boldsymbol{0}_3 & \boldsymbol{0}_3 \end{bmatrix} \quad \boldsymbol{\Gamma} = \begin{bmatrix} \boldsymbol{\Gamma}_{11} & \boldsymbol{0}_3 \\ \boldsymbol{0}_3 & \boldsymbol{\Gamma}_{22} \\ \boldsymbol{0}_3 & \boldsymbol{0}_3 \\ \boldsymbol{0}_3 & \boldsymbol{0}_3 \end{bmatrix} \tag{12}$$

$$\boldsymbol{H} = \begin{bmatrix} \boldsymbol{E}_3 & \boldsymbol{0}_{3\times 2} & \boldsymbol{0}_{3\times 1} & \boldsymbol{0}_{3\times 6} \\ \boldsymbol{0}_{1\times 3} & \boldsymbol{0}_{1\times 2} & 1 & \boldsymbol{0}_{1\times 6} \end{bmatrix}$$

)where $\boldsymbol{0}_{m\times n} \in \boldsymbol{R}^{m\times n}$ and each elements in $\boldsymbol{0}_{m\times n}$ is 0.

3.3 Uncertain Vibrations Coupled in IMU Outputs

The effect of vibrations on the angular rate and the acceleration is investigated by Jan and Shau-Shiun (Jan, 2011), who show that the acceleration is corrupted by vibrations more severely than the angular rate. Filters are the most popular methods to relieve the vibration's influence. However, filters can work well only if the frequency of the noise is far away from the signal band width. The empirical signal band width of the acceleration is less than 0.4Hz at the sampling rate of 50Hz, which is far away from the vibration frequency [3.33~18.33] Hz. The principal vibration in the acceleration can be treated as a simple sinusoidal axial vibration. Thus the input is modeled as.

$$n_x^t = n_x^m + \delta n_x + a\sin(\varpi t + \varphi_0) + \omega_x \tag{13}$$

The third part on the right side of the equal sign shows the uncertain vibration. As the vibration depends on magnitude a, frequency ϖ and phase φ entirely, it is well-deserved to set $[a\ \varpi\ \varphi]^{\mathrm{T}}$ as the state to determine the

vibration. The vibration parameters dynamic is

$$\begin{bmatrix} \dot{a} \\ \dot{\varpi} \\ \dot{\varphi} \end{bmatrix} = \begin{bmatrix} 0 & 0 & 0 \\ 0 & 0 & 0 \\ 0 & 1 & 0 \end{bmatrix} \begin{bmatrix} a \\ \varpi \\ \varphi \end{bmatrix} \tag{14}$$

Similarly, the estimation model is established by augmenting vibration parameters to the prior state, that is $[v^n\ v^e\ v^d\ \phi\ \theta\ \psi\ \delta n_x\ \delta n_y\ \delta n_z\ \delta p\ \delta q\ \delta r\ a\ \varpi\ \varphi]^{\mathrm{T}}$. The corresponding Jacobian matrices for the attitude determination with considering vibration is.

$$\boldsymbol{F} = \begin{bmatrix} \boldsymbol{0}_3 & \boldsymbol{F}_{12} & \boldsymbol{\Gamma}_{11} & \boldsymbol{0}_3 & \boldsymbol{F}_{15} \\ \boldsymbol{0}_3 & \boldsymbol{F}_{22} & \boldsymbol{0}_3 & \boldsymbol{\Gamma}_{22} & \boldsymbol{0}_3 \\ \boldsymbol{0}_3 & \boldsymbol{0}_3 & \boldsymbol{0}_3 & \boldsymbol{0}_3 & \boldsymbol{0}_3 \\ \boldsymbol{0}_3 & \boldsymbol{0}_3 & \boldsymbol{0}_3 & \boldsymbol{0}_3 & \boldsymbol{0}_3 \\ \boldsymbol{0}_3 & \boldsymbol{0}_3 & \boldsymbol{0}_3 & \boldsymbol{0}_3 & \boldsymbol{F}_{55} \end{bmatrix} \quad \boldsymbol{\Gamma} = \begin{bmatrix} \boldsymbol{\Gamma}_{11} & \boldsymbol{0}_3 \\ \boldsymbol{0}_3 & \boldsymbol{\Gamma}_{22} \\ \boldsymbol{0}_{9\times3} & \boldsymbol{0}_{9\times3} \end{bmatrix} \tag{15}$$

$$\boldsymbol{H} = \begin{bmatrix} \boldsymbol{E}_3 & \boldsymbol{0}_{3\times2} & \boldsymbol{0}_{3\times1} & \boldsymbol{0}_{3\times9} \\ \boldsymbol{0}_{1\times3} & \boldsymbol{0}_{1\times2} & 1 & \boldsymbol{0}_{1\times9} \end{bmatrix}$$

where $g\begin{bmatrix} s_\phi c_\psi c_\theta & 0 & ac_\phi c_\psi c_\theta \\ s_\phi s_\psi c_\theta & 0 & ac_\phi s_\psi c_\theta \\ -s_\phi s_\theta & 0 & -as_\phi s_\theta \end{bmatrix}$ and $\begin{bmatrix} 0 & 0 & 0 \\ 0 & 0 & 0 \\ 0 & 1 & 0 \end{bmatrix}$ are defined for $\boldsymbol{F}_{15}$ and $\boldsymbol{F}_{55}$, respectively.

3.4 Hybrid EKF for Dual Estimation

Attitude and unknown parameters are augmented as states in hybrid EKF. It is significant to show that the dynamics is continuous with time, while the observation is gotten by sampling. Compared with continuous and discrete EKF, hybrid EKF is the optimum dual estimation method for the hybrid model. Hybrid EKF is the combination of continuous EKF and discrete EKF. In the time-update step, there is no observed information for the reference, thus the observation variance should be set infinite at the moment [21]. Therefore, the states are propagated with no innovations when the observed variance is set infinite. In the measurement-update step, the principal process is to update states and the error variance according to the measurement-update step of discrete EKF. With the above discuss, the Hybrid EKF can be programmed on the following steps.

Initial Step: For k=0, initialize the initial state $\boldsymbol{x}_0$ and the initial error variance $\boldsymbol{P}_0$. For k=1,2,…, execute the following steps repeatedly.

Time-update Step: Propagate $\hat{\boldsymbol{x}}_{k,k-1}$ and $\boldsymbol{P}_{k,k-1}$ by the forth-order Runge-Kutta integration with $\hat{\boldsymbol{x}}_{k-1}$ and $\boldsymbol{P}_{k-1}$ as initials. The time-update equations for $\hat{\boldsymbol{x}}_{k,k-1}$ and $\boldsymbol{P}_{k,k-1}$ are

$$\begin{cases} \dot{\boldsymbol{x}} = \boldsymbol{f}(\boldsymbol{x}, \boldsymbol{u}^{\mathrm{m}}) \\ \dot{\boldsymbol{P}} = \boldsymbol{F}\boldsymbol{P} + \boldsymbol{P}\boldsymbol{F}^{\mathrm{T}} + \boldsymbol{\Gamma}\boldsymbol{Q}\boldsymbol{\Gamma}^{\mathrm{T}} \end{cases} \tag{16}$$

Measurement-update Step: Update $\hat{\boldsymbol{x}}_k$ and $\boldsymbol{P}_k$ when measurement is available. The measurement-update equation is

$$\begin{cases} \boldsymbol{K}_k = \boldsymbol{P}_{k,k-1}\boldsymbol{H}^{\mathrm{T}}(\boldsymbol{H}\boldsymbol{P}_{k,k-1}\boldsymbol{H}^{\mathrm{T}} + \boldsymbol{R})^{-1} \\ \hat{\boldsymbol{x}}_k = \hat{\boldsymbol{x}}_{k,k-1} + \boldsymbol{K}_k(\boldsymbol{z}_k - \boldsymbol{h}(\hat{\boldsymbol{x}}_{k,k-1})) \\ \boldsymbol{P}_k = (\boldsymbol{E}_{15} - \boldsymbol{K}_k\boldsymbol{H})\boldsymbol{P}_{k,k-1} \end{cases} \tag{17}$$

3.5 State and Parameters Separated Estimation

The joint hybrid EKF for states and parameters dual estimation needs to calculate a high order matrix when calculating $\boldsymbol{P}_{k,k-1}$, $\boldsymbol{K}_k$ and $\boldsymbol{P}_k$. The operation of the high order matrix requires the large storage and immense amount of calculation. As a result, the stability and the accuracy of the filter are prone to be degraded by any numerical solver. In order to realize the state and parameters separated estimation, the joint state should be classified into three categories, including the basic state $\boldsymbol{x} = [v^n\ v^e\ v^d\ \phi\ \theta\ \psi]^{\mathrm{T}}$, the uncertain constant bias $\boldsymbol{b} = [\delta n_x\ \delta n_y\ \delta n_z\ \delta p\ \delta q\ \delta r]^{\mathrm{T}}$ and the uncertain vibration parameters $\boldsymbol{v} = [a\ \varpi\ \varphi]^{\mathrm{T}}$. Meanwhile, the error variance $\boldsymbol{P}$, dynamic matrix $\boldsymbol{F}$, process noise mapping matrix $\boldsymbol{\Gamma}$ and measurement matrix $\boldsymbol{H}$ are partitioned as following.

$$\boldsymbol{P} = \begin{bmatrix} \boldsymbol{P}_{\mathrm{x}} & \boldsymbol{P}_{\mathrm{xb}} & \boldsymbol{P}_{\mathrm{xv}} \\ \boldsymbol{P}_{\mathrm{xb}}^{\mathrm{T}} & \boldsymbol{P}_{\mathrm{b}} & \boldsymbol{P}_{\mathrm{bv}} \\ \boldsymbol{P}_{\mathrm{xv}}^{\mathrm{T}} & \boldsymbol{P}_{\mathrm{bv}}^{\mathrm{T}} & \boldsymbol{P}_{\mathrm{v}} \end{bmatrix} \quad \boldsymbol{F} = \begin{bmatrix} \boldsymbol{F}_{\mathrm{xx}} & \boldsymbol{F}_{\mathrm{xb}} & \boldsymbol{F}_{\mathrm{xv}} \\ \boldsymbol{0}_6 & \boldsymbol{0}_6 & \boldsymbol{0}_{6\times3} \\ \boldsymbol{0}_{3\times6} & \boldsymbol{0}_{3\times6} & \boldsymbol{F}_{\mathrm{vv}} \end{bmatrix}$$

$$\boldsymbol{\Gamma}^{\mathrm{T}} = \begin{bmatrix} \boldsymbol{\Gamma}_{\mathrm{x}}^{\mathrm{T}} & \boldsymbol{0}_6 & \boldsymbol{0}_3 \end{bmatrix}^{\mathrm{T}} \quad \boldsymbol{H} = \begin{bmatrix} \boldsymbol{H}_{\mathrm{x}} & \boldsymbol{0}_{4\times6} & \boldsymbol{0}_{4\times3} \end{bmatrix}$$

According to the matrix blocking theorem the partitioned error variance propagation matrix, Kalman gain matrix and error variance update matrix should be updated as equations (18~20).

$$\begin{cases} \dot{\boldsymbol{P}}_{\mathrm{x}} = \boldsymbol{F}_{\mathrm{xx}}\boldsymbol{P}_{\mathrm{x}} + \boldsymbol{F}_{\mathrm{xb}}\boldsymbol{P}_{\mathrm{xb}}^{\mathrm{T}} + \boldsymbol{F}_{\mathrm{xv}}\boldsymbol{P}_{\mathrm{xv}}^{\mathrm{T}} + \boldsymbol{P}_{\mathrm{x}}\boldsymbol{F}_{\mathrm{xx}}^{\mathrm{T}} + \boldsymbol{P}_{\mathrm{xb}}\boldsymbol{F}_{\mathrm{xb}}^{\mathrm{T}} \\ \qquad + \boldsymbol{P}_{\mathrm{xv}}\boldsymbol{F}_{\mathrm{xv}}^{\mathrm{T}} + \boldsymbol{\Gamma}_{\mathrm{x}}\boldsymbol{Q}\boldsymbol{\Gamma}_{\mathrm{x}}^{\mathrm{T}} \\ \dot{\boldsymbol{P}}_{\mathrm{b}} = \boldsymbol{0}_6 \\ \dot{\boldsymbol{P}}_{\mathrm{v}} = \boldsymbol{F}_{\mathrm{vv}}\boldsymbol{P}_{\mathrm{v}} + \boldsymbol{P}_{\mathrm{v}}\boldsymbol{F}_{\mathrm{vv}}^{\mathrm{T}} \end{cases} \tag{18}$$

$$\begin{cases} \boldsymbol{K}_{\mathrm{k}}^{\mathrm{x}} = \boldsymbol{P}_{\mathrm{x}}\boldsymbol{H}_{\mathrm{x}}^{\mathrm{T}}(\boldsymbol{H}_{\mathrm{x}}\boldsymbol{P}_{\mathrm{x}}\boldsymbol{H}_{\mathrm{x}}^{\mathrm{T}} + \boldsymbol{R})^{-1} \\ \boldsymbol{K}_{\mathrm{k}}^{\mathrm{b}} = \boldsymbol{P}_{\mathrm{xb}}^{\mathrm{T}}\boldsymbol{H}_{\mathrm{x}}^{\mathrm{T}}(\boldsymbol{H}_{\mathrm{x}}\boldsymbol{P}_{\mathrm{x}}\boldsymbol{H}_{\mathrm{x}}^{\mathrm{T}} + \boldsymbol{R})^{-1} \\ \boldsymbol{K}_{\mathrm{k}}^{\mathrm{v}} = \boldsymbol{P}_{\mathrm{xv}}^{\mathrm{T}}\boldsymbol{H}_{\mathrm{x}}^{\mathrm{T}}(\boldsymbol{H}_{\mathrm{x}}\boldsymbol{P}_{\mathrm{x}}\boldsymbol{H}_{\mathrm{x}}^{\mathrm{T}} + \boldsymbol{R})^{-1} \end{cases} \tag{19}$$

$$\begin{cases} \boldsymbol{P}_{\mathrm{k}}^{\mathrm{x}} = \boldsymbol{P}_{\mathrm{x}} - \boldsymbol{K}_{\mathrm{k}}^{\mathrm{x}}\boldsymbol{H}_{\mathrm{x}}\boldsymbol{P}_{\mathrm{x}} \\ \boldsymbol{P}_{\mathrm{k}}^{\mathrm{b}} = \boldsymbol{P}_{\mathrm{b}} - \boldsymbol{K}_{k}^{\mathrm{b}}\boldsymbol{H}_{\mathrm{x}}\boldsymbol{P}_{\mathrm{xb}} \\ \boldsymbol{P}_{\mathrm{k}}^{\mathrm{v}} = \boldsymbol{P}_{\mathrm{v}} - \boldsymbol{K}_{k}^{\mathrm{v}}\boldsymbol{H}_{\mathrm{x}}\boldsymbol{P}_{\mathrm{xv}} \end{cases} \tag{20}$$

Meanwhile, three time-update covariance matrices and three measurement-update covariance matrices are induced in the state and parameters separated estimation. They are propagated and updated by Eq. (21) and Eq. (22), respectively.

$$\begin{cases} \dot{\boldsymbol{P}}_{\mathrm{xb}} = \boldsymbol{F}_{\mathrm{xx}}\boldsymbol{P}_{\mathrm{xb}} + \boldsymbol{F}_{\mathrm{xb}}\boldsymbol{P}_{\mathrm{b}} + \boldsymbol{F}_{\mathrm{xv}}\boldsymbol{P}_{\mathrm{bv}}^{\mathrm{T}} \\ \dot{\boldsymbol{P}}_{\mathrm{xv}} = \boldsymbol{F}_{\mathrm{xx}}\boldsymbol{P}_{\mathrm{xv}} + \boldsymbol{F}_{\mathrm{xb}}\boldsymbol{P}_{\mathrm{bv}} + \boldsymbol{F}_{\mathrm{xv}}\boldsymbol{P}_{\mathrm{v}} + \boldsymbol{P}_{\mathrm{xv}}\boldsymbol{F}_{\mathrm{vv}}^{\mathrm{T}} \\ \dot{\boldsymbol{P}}_{\mathrm{bv}} = \boldsymbol{P}_{\mathrm{bv}}\boldsymbol{F}_{\mathrm{vv}}^{\mathrm{T}} \end{cases} \tag{21}$$

$$\begin{cases} \boldsymbol{P}_{k}^{\mathrm{xb}} = (\boldsymbol{E}_6 - \boldsymbol{K}_{k}^{\mathrm{x}}\boldsymbol{H}_{\mathrm{x}})\boldsymbol{P}_{\mathrm{xb}} \\ \boldsymbol{P}_{k}^{\mathrm{xv}} = (\boldsymbol{E}_6 - \boldsymbol{K}_{k}^{\mathrm{x}}\boldsymbol{H}_{\mathrm{x}})\boldsymbol{P}_{\mathrm{xv}} \\ \boldsymbol{P}_{k}^{\mathrm{bv}} = \boldsymbol{P}_{\mathrm{bv}} - \boldsymbol{K}_{k}^{\mathrm{b}}\boldsymbol{H}_{\mathrm{x}}\boldsymbol{P}_{\mathrm{xv}} \end{cases} \tag{22}$$

For the time-update step, the basic state is updated by Eq. (1) and Eq. (2) for attitude and velocity. The bias holds its value during the time-update step. Vibration parameters are updated by Eq.(12). For the measurement-update step, the basic state, bias and vibration parameters are calibrated according to Eq. (23), respectively.

$$\hat{\boldsymbol{x}}_k^{\mathbf{j}} = \hat{\boldsymbol{x}}_{k,k-1}^{\mathbf{x}} + \boldsymbol{K}_{\mathbf{k}}^{\mathbf{j}}(z_k - \boldsymbol{h}(\hat{\boldsymbol{x}}_{k,k-1}^{\mathbf{x}})) \quad \mathbf{j} = \mathbf{x}, \mathbf{b}, \mathbf{v} \tag{23}$$

Compared with the joint EKF, the main advantage of state and parameters separated estimation for the dual estimation is the smaller storage and the lower computing loads. The maximum order of matrix in reduced order EKF is 6×6 while the order of general matrix in full order EKF is 15×15. It is deserved to notice that there are three covariance matrices with respect to the portioned state should be propagated and updated in the filter.

4 Presentation of Result

4.1 Simulation Settings

Before simulation, the small UAV is shifted to its balanced state, and then the attitude commands are sent to manipulate UAV to maneuver. Roll, pitch and yaw commands are all set as 10 degrees for 1 seconds, and the command is send to the UAV at the time of 10, 30, 50, 70, 90 second. δn_x, δn_y and δn_z are all set as 0.01g. δp, δq, δr are all set as $0.1\,^{o}/s$. The vibration parameters a, ϖ and φ are set as 1.1g, 3.9Hz and $\pi/3$ radian, respectively. The standard variances of Gaussian white noises in the output of the accelerometer and the gyroscope are 10^{-2} g and $0.5^{o}/s$, respectively. The standard deviations of Gaussian white noises in the measurement are $0.05m/s$ for the velocity and 0.5^{o} for the heading.

4.2 Result discussion

It is essential to define the following formulas to assess the performance of the vibration considered dual estimation for attitude and parameters.

Moving average and standard variance of errors are

$$e_k = \frac{1}{2n+1}\sum_{j=k-n}^{k+n} e_j \quad \sigma_k = \sqrt{\frac{1}{2n}\sum_{j=k-n}^{k+n} e_j^2} \tag{24}$$

Where, n is chosen as 99 in the paper.

Fig. 3 presents curve of the roll attitude versus time, the dash line shows the result deduced by the Dead Reckoning (DR), and the solid line shows the result deduced by Dual Estimation Considering Vibration (DECV). The roll attitude errors of DECV are convergent to the tolerance band. On the contrary, the roll attitude errors of DR are gradually increased with time. The comparison demonstrates that DECV is more suitable to estimate the indirect observed state than DR.

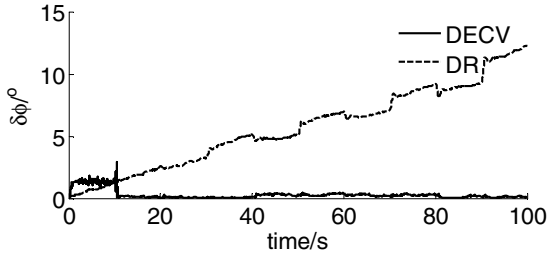

Fig.3 Roll errors of DECV and DR

Fig.4 depicts the heading errors' spectrum of estimation and observation. The observation heading error's spectrum distributes uniformly over all the frequency. The estimation heading error's spectrum is restrained to the lower frequency, while the higher frequency spectrum is approximated to 0. This suggests the hybrid EKF a low-pass filter in nature.

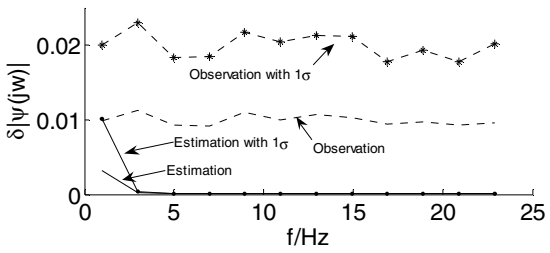

Fig.4 Heading error spectrum of estimation and observation

Fig.5 illustrate error curves of observation and estimation. The moving average errors of estimation and observation are all approximate to 0. However, the region of estimation due to 1σ is much small than that of the observation due to 1σ.

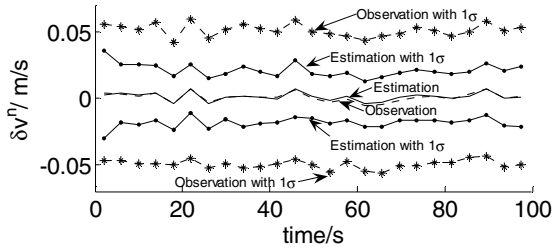

Fig.5 Northern velocity error curves of observation and estimation.

Figures 6- 8 show moving average error and moving average error with 1σ curves of CF estimation and DECV estimation in time domain. The moving average error of CF estimation and DECV estimation are gradually approximate to 0. Without horizontal attitude observation, the beginning estimation errors of horizontal attitude are far away from the truth. After 20s, the error region of CF estimation due to 1σ is almost wider than or same as the region of the DECV estimation due to 1σ.

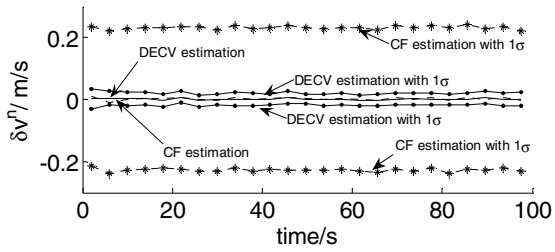

Fig.6 Northern velocity error curves of CF and DECV.

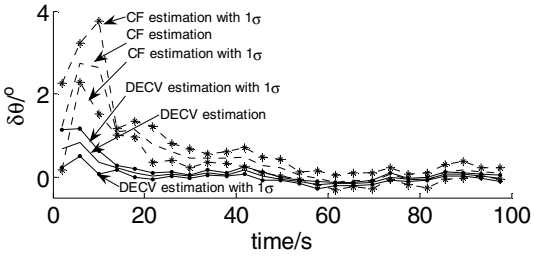

Fig.7 Pitch angle error curves of CF and DECV.

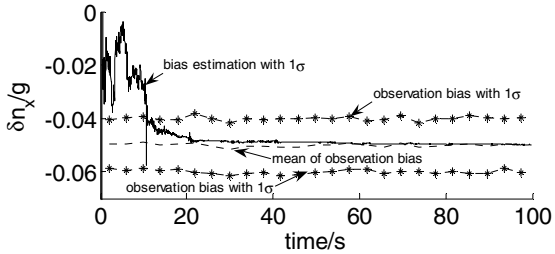

Fig.8 Axial acceleration bias curves of observation and DECV.

Figure 9 shows that the vibration magnitude estimated by DECV is quite close to the truth with 6.15% errors. Figure 10 illustrates that the vibration frequency estimated by DECV is asymptotically approximated to the truth. As Figure 11 shows, the vibration power spectrum is attenuated greatly by DECV at the frequency of 3.9Hz.

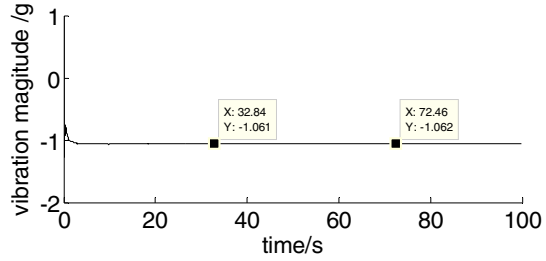

Fig.9 Vibration magnitude estimation with DECV.

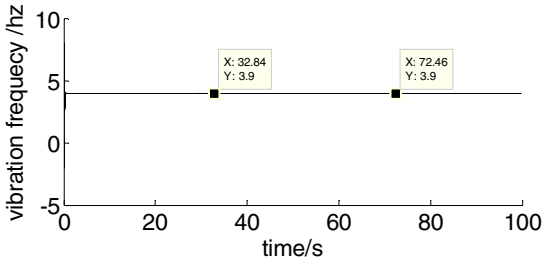

Fig.10 Vibration frequency estimation with DECV.

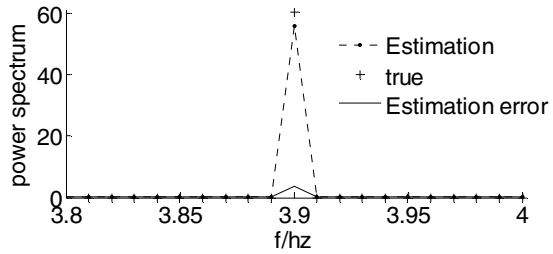

Fig.11 Power spectrum of vibration estimated with DECV.

5 Conclusions

MEMS IMU and GPS are integrated as the priory method for the determination of the UAV attitude, velocity and location. This paper focuses to determine the attitude by IMU and GPS, when the acceleration and angular rate observed by IMU are corrupted with the Gaussian White noise, constant bias and simplex sinusoid vibration, the velocity and heading observed by GPS are corrupted with the Gaussian White noise. The Gaussian White noise make the dead reckoning result with some random uncertain. The constant bias makes the dead reckoning result divergence. The vibration makes the dead reckoning result show unacceptable vibration. By augmenting constant bias and vibration parameters to the basic state of velocity and attitude, the attitude determination problem is transformed to a standard filter problem. By linearizing the system to get the Jacobian matrices, the hybrid EKF is possible to employed to determine the attitude. Simulation result shows that the proposed method is more accurate than the method without considering vibration.

There are still some future works, such as how to determine the attitude when the vibration is treated as a complex sinusoid vibration, or the vibration is treated as a damping sinusoid vibration, *et al*.

References

[1] Kato O. Attitude Projection Method for Analyzing Large-Amplitude Airplane Maneuvers [J]. Journal of Guidance, Control, and Dynamics, 1990, 13(1):22-29.

[2] Gebre-Egziabher D. Design of multi-sensor attitude determination systems [J]. IEEE Transactions on Aerospace and Electronic Systems, 2004, 40(2):627-649.

[3] Zhu R, Zhou Z. A Small Low-Cost Hybrid Orientation System and Its Error Analysis [J]. IEEE Sensors Journal, 2009, 9(3):223-230.

[4] Zhu R, Song D, Zhou Z Y, et al. A linear fusion algorithm for attitude determination using low cost MEMS-based sensors [J]. Measurement, 2007, 40(3):322-328.

[5] Gebre-Egziabher D, Elkaim G H, Powell J D, et al. a Gyro-free quaternion-based attitude determination system suitable for implementation using low cost sensors[J]. Position Location and Navigation Symposium, IEEE 2000, 2000:185-192.

[6] Jan Y, Shau-Shiun L. Attitude estimation based on fusion of gyroscopes and single antenna GPS for small UAVs under the influence of vibration[J]. GPS Solut, 2011, 15(1):67-77.

[7] Gebre-Egziabher D, Elkaim G H. MAV Attitude Determination by Vector Matching [J]. IEEE Transactions on Aerospace and Electronic Systems, 2008, 44(3):1012-1028.

[8] Wahba G. Problem 65-1 (solution)[J]. SIAM, Review, 1966,8:384-386.

[9] Qin L, Zhang W, Zhang H, et al. Attitude measurement system based on micro-silicon accelerometer array[J]. Chaos, Solitons and Fractals, 2006, 29(1):141-147.

[10] Tenn H, Jan S, Hsiao F. Pitch and roll attitude estimation of a small-scaled helicopter using single antenna GPS with gyroscopes[J]. GPS Solutions, 2009, 13(3):209.

[11] Fu X, Zhou Z Y, Xiong S S, Wang J D. MEMS multi-sensor attitude determination system based on the EKF. Journal of Tsinghua University (Science and Technology) 2006; 46(11): 1857-1859, 1863. [In Chinese]

[12] Roskam J. Flight Dynamics and Automatic Flight Controls [G]. The University of Kansas, Lawrence: Design, AIlalysis and Research Corporation, 2001.

[13] Ito K, Xiong K. Gaussian Filters for Nonlinear Filtering Problems [J]. IEEE Transactions on Automatic Control, 2000, 45(5):910-927.

[14] Norgaard M, Poulsen N K, Ravn O. New developments in state estimation for nonlinear systems [J]. Automatica, 2000, 36:1627-1638.

[15] Crassidis J L, Markley F L, Cheng Y. Survey of nonlinear attitude estimation methods [J]. Journal of Guidance, Control, and Dynamics, 2007, 30(1):12-28.

[16] Xu B, Huang X Y, Wang DW, *et al*. Dynamic Surface Control of Constrained Hypersonic Flight Models with Parameter Estimation and Actuator Compensation[J]. Asian Journal of Control, DOI: 10.1002/asjc.679

[17] Xu B, Gao D X,Wang S X. Adaptive neural control based on HGO for hypersonic flight vehicles[J]. Science China Information Sciences, 2011, 54(3):511-520

[18] Xu B, Sun F C, Yang C G, *et al*. Adaptive Discrete-time Controller Design with Neural Network for Hypersonic Flight Vehicle via Back-stepping[J]. International Journal of Control, 2011, 84(9):1543-1552

[19] Xu B, Sun F C, Liu H P, *et al*. Adaptive Kriging Controller Design for Hypersonic Flight Vehicle via Back-stepping[J]. IET Control Theory and Applications, 2012,6(4): 487-497

[20] Xu B, Wang D W, Sun F C*, et a*l. Direct Neural Discrete Control of Hypersonic Flight Vehicle[J]. Nonlinear Dynamics , 2012, 70(1): 269–278

[21] Simon D. optimal state estimation [M]. A John Wiley & Sons, Inc., Publication, 2006.